Available online at www.sciencedirect.com

ScienceDirect

Journal of Ocean Engineering and Science 1 (2016) 77–83

www.elsevier.com/locate/joes

Experimental studies on the flow characteristics in an inclined bend-free OWC device

Krishnil Ravinesh Ram[a], Mohammed Rafiuddin Ahmed[a,*], Mohammed Asid Zullah[b], Young-Ho Lee[b]

[a] *Division of Mechanical Engineering, The University of the South Pacific, Suva, Fiji*
[b] *Division of Mechanical and Energy System Engineering, Korean Maritime and Ocean University, Busan, Republic of Korea*

Received 8 July 2015; received in revised form 28 September 2015; accepted 8 October 2015
Available online 3 February 2016

Abstract

A bend-free rectangular cross-section OWC device was designed and constructed for studying the effect of inclination on the flow characteristics inside the device. The inclination is meant to reduce reflection of waves and induce higher velocities in the turbine section. Experimental measurements were made in a wave channel where the OWC device was tested. An S-type Pitot tube was used to measure dynamic pressure of air in the turbine section at several inclinations. Particle Image Velocimetry (PIV) was also done to study the flow of both air and water in the OWC device. In order to focus solely on primary energy capture, no turbine was installed in the OWC device. The dynamic pressure readings were analysed for suction and compression stages. Water volume fluctuations inside the capture chamber were also recorded and compared for different inclinations. The result was an increase in the velocity of air flowing in the capture chamber and hence a rise in the kinetic energy available to the turbine. It was found from experimental studies that as the angle of inclination reduced, the velocity of air in the turbine section increased. The lower angles also caused higher run-up and larger volume of water into the capture chamber.

Keywords: Oscillating water column; Particle Image Velocimetry; Wave energy.

1. Introduction

Wave energy can be considered as a concentrated form of solar energy [2,30]. Solar heating causes wind-flow due to temperature difference, which in turn creates the waves in the sea. The global wave power resource in water depths of over 100 m has been estimated as between 1 and 10 TW, while the economically exploitable resource ranges from 140 to 750 TW h/yr for current designs when fully mature, and could be as high as 2000 TW h/yr if the potential improvements to existing devices are achieved [30]. The power in a wave can be computed using the following equation [8]:

$$P = \frac{1}{8}\rho g H^2 c_g \tag{1}$$

where c_g is defined for any finite depth of water as:

$$c_g = \frac{1}{2}\left[1 + \frac{2kh}{\sinh 2kh}\right]\frac{gT}{2\pi}\tanh(kh) \tag{2}$$

There are many devices that can extract energy from the waves. The devices can be grouped into two main classes: (1) off-shore devices based on floating articulated bodies oscillating under the action of waves and (2) near-shore and on-shore devices based on the conversion of wave motion into oscillating air flow driving a turbine [28]. The response of a wave energy device is generally frequency dependent. The peak (resonant) frequency and the range of frequencies that will produce a significant response will depend on the particular device [29].

* Corresponding author: Tel.: +679 3232042; fax: +679 3231538.
E-mail address: ahmed_r@usp.ac.fj, ahmedm1@asme.org (M.R. Ahmed).

http://dx.doi.org/10.1016/j.joes.2015.12.003

Nomenclature

ρ	water density, kg/m^3
g	gravitational acceleration, m/s^2
H	wave height, m
T	wave period, s
k	wave number
h	water depth, m
K_r	reflection coefficient
r_r	slope roughness co-efficient
N_i	surf similarity parameter (Iribarren number)
T_p	peak wave period, s

The oscillating water column (OWC) is one of the most widely researched and promising wave energy devices [5,6,15,21,25]. As the wave impinges on the OWC device, it causes oscillation of the free water surface in the capture chamber, which in turn causes bi-directional air flow in the upper part of the OWC device. An appropriate bi-directional turbine can be used to convert this kinetic energy to electricity. Capable of operating in reversing flow conditions, the Wells turbine is generally used to avoid the addition of rectifying valves to correct one of the flow phases [3]. Impulse turbines capable of self-rectification have been studied in detail for use in OWCs by [16] and others. Cross flow turbines such as Savonius rotors have also been proposed [4,14,19].

The OWC can be fixed or floating type. The present study was performed on a fixed type OWC. There are several fixed OWC plants built. To reduce capital cost, fixed type OWCs are normally integrated within harbour breakwaters. However, a fixed OWC offers advantages such as extended life, easier maintenance and cost sharing with shore protection structures. Design parameters of shallow depth fixed OWCs are discussed by [11]. In moderate wave climates, the need to improve primary energy capture plays a crucial role in the viability of an OWC system. Zaoui et al. [31] opined that due to numerical accuracy problem near the wave-structure interaction zone, lab experimental work is of paramount importance and gives confidence to investors and governments in this upcoming technology.

A feature of a fixed type OWC is that the depth and consequently the wave heights will be limited. The water particles follow elliptical orbits in shallow and intermediate depth waters [7]. The horizontal components of the particle velocity are greater and in the direction of propagation; as the wave impacts a vertical wall, most of the particles will reflect away from the vertical wall and not upwards towards the air duct. This is typical of many conventional OWCs. Front wall has similar effects. There have been many studies done on reflection of waves from vertical and inclined walls [13,23,26,27]. During reflection from a vertical rigid wall, a partially standing wave is formed in front of the vertical structure, which has the combined amplitude of the incident and reflected waves [7,9]. The front wall of the OWC distorts this partially standing wave and the effect of the increased amplitude is reduced. In most cases, the reflected wave superimposes on the incoming wave and causes a net reduction in wave height. In the vertical chamber, the rear wall provides a barrier and does not guide the near horizontal velocities in the upward direction. Just as it would reduce work on a solid object moving up, the incline aids the bulk volume of water to rise into the capture chamber, rather than reflecting it. Reflections from sloping structures are less severe than from vertical walls [26,1].

So far, there has been only the LIMPET OWC that uses inclined walls in its capture chamber. The inclined column offers an easier path for water ingress and egress resulting in less turbulence and lower energy loss. This is particularly true at the shoreline where shallow water effects have increased the surge motions relative to heave [9].

This paper discusses the effect of inclination of the front and rear walls of the capture chamber on the energy available to the turbine. The water volume change inside the chamber for different inclinations is also studied.

2. Experimental method

The experiments were carried out on a wave channel that is 3.5 m long, 0.3 m wide and 0.45 m deep, and uses a flap type wave maker hinged at the bottom to generate sinusoidal waves. The close fit of the wave maker to the wave channel sides ensures that two-dimensional waves are produced with no fluid motion normal to the sidewalls [20]. Controlling the frequency of the wave maker simulates different sea states of various periods. Fig. 1 gives a schematic of the wave channel. The water flow is generated by a centrifugal pump having a rated capacity of 40 l/s at a total head of 10 m and driven by a 5.5 kW motor. The pump draws water from a tank of 1.5 m x 0.8 m cross-section which receives back the same water from the wave channel.

A Cussons Tuneable Beach, model P6285, was placed at the other end of the wave channel. The beach consists of a series of porous plates with different porosity levels to absorb the wave energy gradually and minimise reflections.

The OWC device model was built out of clear Perspex to a scale of 1:60. The experimental OWC device is made bend-free to prevent losses due to bending of the duct and also for ease of comparison of results. The device has a rectangular capture chamber that is connected to a circular turbine section via a transition duct. The transition allows an obstacle free path to the airflow and reduces energy losses at the duct

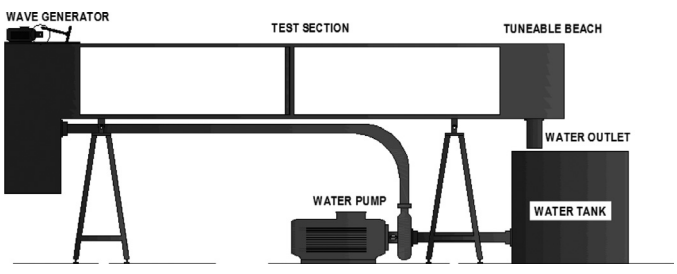

Fig. 1. Schematic diagram of the wave channel.

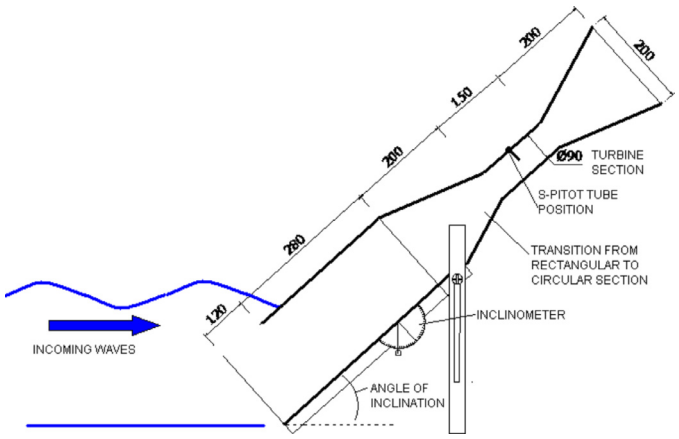

Fig. 2. Schematic diagram of the inclined OWC device.

walls due to abrupt shape changes. Fig. 2 shows a schematic diagram of the OWC device. To avoid comparisons of different material usage in construction, a single OWC device was hinged onto two side supports that allow the OWC to change its inclination angle. A side-mounted inclinometer was used to set the correct angle. The OWC device was designed to cover almost the entire width of the wave channel to allow two-dimensional analysis. An aluminium frame was used to secure the setup. An S-Pitot tube which was fabricated in-house and calibrated against a standard Pitot-static tube was inserted at the location indicated in Fig. 2. A Furness Controls, FCO510 model, digital micro-manometer with a range of ±200 mm of water was used to measure the differential pressure.

To determine the conditions of the waves created in the wave channel and the relationships between various parameters, Seiki pressure transducers, model PSHF002KAAG, were used to measure the wave parameters. The pressure signals were acquired on a GL500A midi-LOGGER dual data logger and analysed to determine the period, wave height and wavelength. For the entire experiment, the water depth was kept constant at 260 mm. The surf similarity parameter and reflection coefficient were also calculated from these data.

Particle Image Velocimetry (PIV) was performed to better understand the airflow in the turbine duct and water interactions with the capture chamber. Vinyl Chloride tracer particles, with an average diameter of 100 μm and a specific gravity of 1.02, were seeded in the water, while pine powder with average particle size of 10 μm was used for air velocity measurements. A 1 W air-cooled solid-state continuous laser with a wavelength of 532 nm was used to illuminate the seeded particles. The motion of the particles was captured by a high-speed *Photron* CCD camera. The camera recorded 125 frames per second, producing up to 1280 × 1024 pixel images. The images captured by the CCD camera were processed using *Cactus 3.3* software.

Fig. 3 shows the PIV set-up and the wave channel. With the depth constant, the frequency of the wave maker was varied from 0.5 to 0.9 Hz to simulate different waves. The OWC

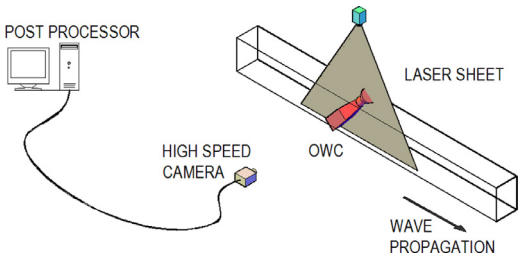

Fig. 3. Schematic diagram of the PIV setup.

was tested at inclination angles of 45°, 55°, 65°, 75° and 90°. Angles of less than 45° proved difficult to test with the same model as the wave run-up reached the turbine section. This would require construction of a longer capture chamber that could prove uneconomical in real situations. Dynamic pressure readings from the turbine section were recorded by logging the dynamic pressure signal every 300 ms using the FC0510 micromanometer. The pressure readings were taken from $t = 0$ which corresponds to the instant when the wave maker starts on the desired frequency. The volume change of the water inside the inclined capture chamber caused by the oscillation of the water surface was noted by marking the maximum rise and minimal fall of the water level in the OWC.

The accuracy of pressure measurements in the present work was estimated to be 2.4%. The repeatability of pressure measurements was within ±1.9%. The factors which were considered for determining the accuracy of velocity measurements with PIV are: the uncertainties due to finite time sampling, finite displacement of the particles, and uncertainties in measuring the displacements of the particle images [18]. The accuracy of displacement measurements with *Cactus* is of the order of 0.1 pixel. For the high speed camera, the time resolution for the current measurements was 0.008 s. To get an accurate estimate of the uncertainty in our measurements, most of which were for rotating (orbital) motion of particles, PIV measurements were performed on a calibrated, constant speed rotating motion and the maximum error was found to be 0.32%.

3. Results and discussion

Fig. 4 shows the wavemaker frequencies in the wave channel and the corresponding wave heights for a depth of 260 mm.

The reflection coefficient was estimated for the different cases studied. The reflection co-efficient is defined as the ratio of the reflected wave energy to the incident wave energy. In this study wave reflection co-efficient (K_r) is calculated from the equation derived by Seelig [22]:

$$K_r = r_r \cdot \tanh(0.1N_i^2) \tag{3}$$

where r_r can be taken as 1.0 for a smooth slope and N_i is the surf similarity parameter or Iribarren number defined by

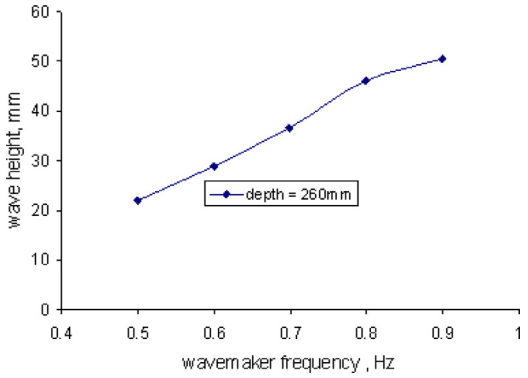

Fig. 4. Wave heights in the wave channel at different frequencies of the wave maker.

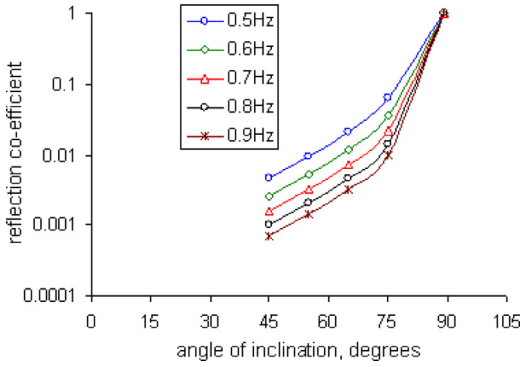

Fig. 5. Reflection coefficient for different angles of inclination at various frequencies.

Jentse and Janssen [10] as:

$$N_i = \frac{\tan\alpha}{\sqrt{\frac{2\pi H_s}{gT_p^2}}} \tag{4}$$

The term in the denominator of Eq. (4) defines the wave steepness parameter while the angle of inclination (α) is in the numerator. The wave height, period and angle of inclination were used to calculate the reflection coefficient. Fig. 5 shows the values of reflection coefficient (on a log scale in y-axis) against the angle of inclination. In the case of the 90° angle, the value of 89° was used since tan of 90° is undefined (this will not have a significant effect on K_r because its maximum value does not exceed unity). The reflection co-efficient increases slightly from 45° to 75°. A dramatic rise in the reflection coefficient to almost 1 occurs at 89°. This semi-empirical result shows a reduction in reflection co-efficient as the angle of inclination of the OWC wall reduces.

Fig. 6 shows representative dynamic pressure variations for three inclination angles at 0.8 Hz. The dynamic pressure in the chamber was measured using an S-type Pitot tube that accurately measures both negative and positive pressure values. The dynamic pressure is derived from the differential pressure output of the digital manometer using the calibration results against the standard Pitot-static tube. The figure clearly shows the difference in the dynamic pressures for the same wave conditions but at different inclination angles. At

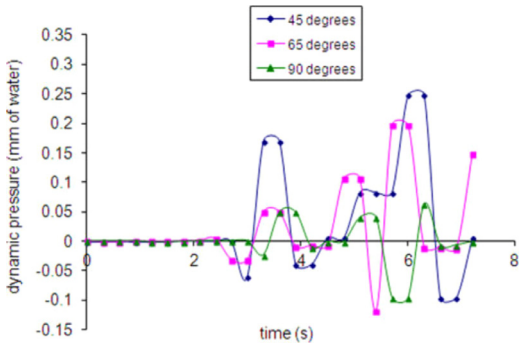

Fig. 6. Representative dynamic pressure variations for three inclination angles at 0.8 Hz. The readings were taken during the first 7 s.

$t = 0$, the dynamic pressure for all the angles is almost zero. While the waves had already been created they did not reach the device until 3 s later. After about 3 s, as the chamber oscillations start, the dynamic pressure starts to increase. It reaches a maximum value before the oscillations stabilise and cause slightly reduced dynamic pressures afterwards. In some cases, the peaks occurred later in time as the oscillations progressed. The values for the vertical OWC position (90°) oscillate mostly between ±0.1 mm of water. The 65° inclination causes the dynamic pressure range to increase to ±0.2 mm, while inclining at 45° results in even higher dynamic pressure values over ±0.25 mm of water. All the readings were restricted to the first few seconds to avoid recording any erroneous readings due to possible reflection of waves from the OWC.

Compared with the vertical OWC, the dynamic pressure is found to improve by about 200% in the 55° configuration. As the angle reduces from 55° to 45°, the dynamic pressures improve by about 33.3%. The dynamic pressure is an indication of the kinetic energy available to the turbine while the amplitude of the wave indicated the energy available to the capture chamber. Similar results were obtained for 0.5 Hz, 0.6 Hz, 0.7 Hz and 0.9 Hz at all angles. Dynamic pressure values are higher in the exhalation or compression stage than in the suction stage in majority of the cases although in some cases the dominance alternates. Similar results have been reported in other works on OWC [19,24].

A parameter used to compare the performance of various pneumatic wave power devices is the air pressure ratio [17]. This is the ratio of the amplitude of pressure divided by the wave height. For all the cases, the maximum amplitude of the dynamic pressure head P_{dyn} was used. H is the wave height in mm.

$$pressureratio = \frac{P_{dyn}}{H} \tag{5}$$

Using the pressure ratio, a comparison can be made for various inclinations of the OWC capture chamber.

Fig. 7 shows the variation of pressure ratio with angle of inclination during the exhalation stage. It is clearly seen that lower angles of inclination yield higher pressure ratios. While the wave conditions vary uniformly with the frequency, the values of pressure ratio peak at 0.8 Hz frequency. The

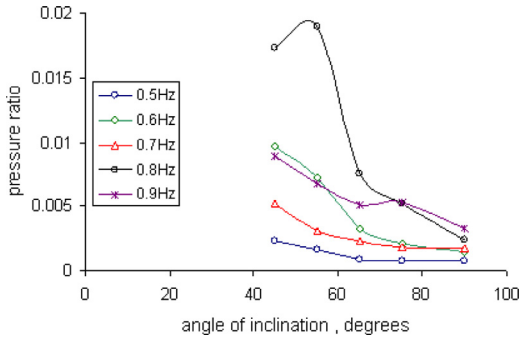

Fig. 7. Peak pressure ratios in the turbine section during the exhalation stage at different inclinations.

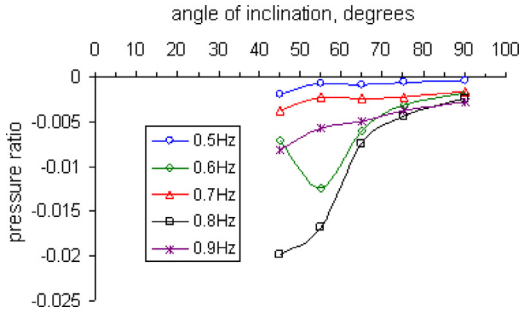

Fig. 8. Peak pressure ratios in the turbine section during the inhalation stage at different inclinations (the negative values indicate reversed direction).

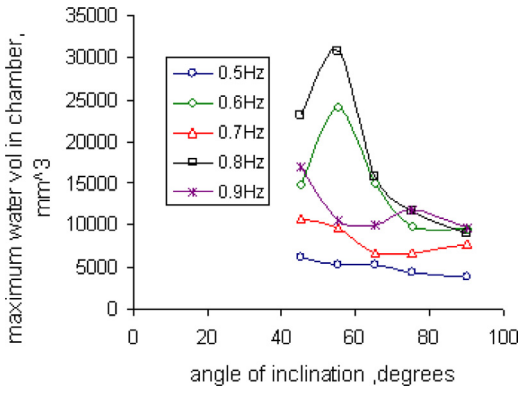

Fig. 9. Water volume fluctuations in the chamber.

favourable results for the 0.8 Hz are also found in water volume fluctuations inside the capture chamber. The oscillations may be well-tuned to the frequency of interaction of the waves with the wavemaker frequency, hence the favourable results. For the same set of experiments the peak pressure ratios during suction (Fig. 8) show similar trend as that with exhalation pressures. Since dynamic pressure is proportional to the velocity of the air, it gives a fair indication of the kinetic energy available to the turbine. The increased velocity in the turbine section provides greater kinetic energy for the air turbine at lower angles. There appears to be a slight increase in velocities from 90° to 65° with a significant increase afterwards until 45°. The anomaly of the 55° inclinations is that at 0.6Hz the suction dynamic pressure is larger than that at 45°. This is repeated for the 0.8 Hz case. The anomaly cannot be experimental error as the water volume flux in the chamber also exhibits similar behaviour as seen in Fig. 9.

At the frequencies of 0.6 Hz and 0.8 Hz, the 55° angles provides a larger volume change in the capture chamber, thus resulting in increased dynamic pressure for the 55° inclinations at the two frequencies. Apart from that the trends in dynamic pressure indicate that as the angle of inclination is reduced from 90° to 45°, the velocity in the turbine duct increases. This means that greater kinetic energy will be available to the turbine after primary conversion. When the wave hits the vertically positioned wall, majority of the wave particles are reflected against the direction of wave propagation while the remaining fluid rises up the capture chamber. The reflected waves superimpose on the incoming incident waves and depending on the reflection co-efficient, reduce the incident wave height. This is the case of the 90° wall. As the wall becomes inclined and the angle of inclination reduces, the reflection coefficient reduces [26]. This is also confirmed by Fig. 5. At lower angles with less reflection, more of the fluid is allowed to rise inside the capture chamber causing a rise in the dynamic pressure values both in the suction and exhalation stages. Sarmento's [21] experimental results showed that for asymmetrically vertical walled OWC the reflection coefficients adversely affect the efficiency [21]. The water volume flux in the capture chamber (Fig. 9) also increases at lower angles when compared to a purely vertical wall. Inclining the device also allows a larger vertical water plane area for entry into the capture chamber. However, the transmission of the surging wave (with the aid of an incline) into the up-chamber direction and reduction of reflection of the incoming wave is the main reason for increased dynamic pressures at lower angles. The reduced reflections allow more water to fill the capture chamber and thus more energy is transmitted to the oscillating air. The volume rise is due to a rise in the free surface height of the water in the capture chamber during wave action. Kwon and Koo [12] simulated a land-based OWC with various pneumatic chamber conditions and evaluated the effect of chamber shape on the energy conversion efficiency.

Fig. 10 shows the behaviour of water particles incident on a 75° inclination of the device. The incoming wave impinges on the front wall and cause run-up on the front wall. Much of the wave is transmitted under the lip of the front wall. The impact merely causes the fluid to rise and then move in the downward direction to the opening. Near the toe of the rear wall the incoming particles travel almost horizontally and upon impact on the rear wall, the particles rise in a direction parallel to the rear wall.

Vortex generation just after the lip can be noticed as well. Such behaviour near the lip of the OWC front wall has also been reported by Jeng [9] for vertical wall lips. There are no such studies for inclined front walls. Similar results are seen for the 45° inclinations at 0.7 Hz in Fig. 11. The incoming particles having a near horizontal velocity travel upwards after impact on the rear wall.

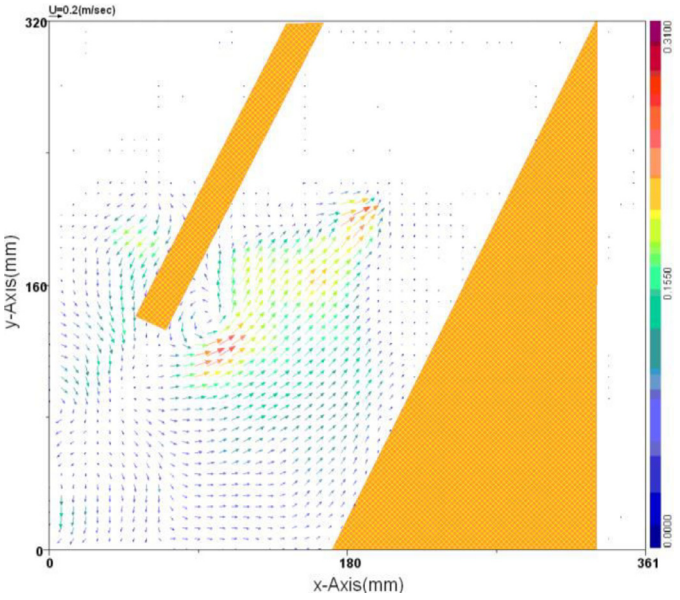

Fig. 10. Velocity vectors showing the motion of water particles for 75° inclination at 0.9 Hz.

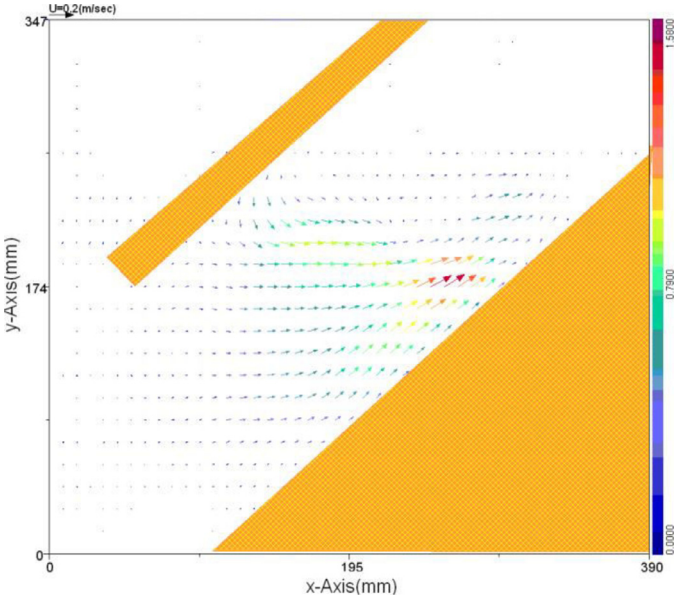

Fig. 11. Velocity vectors showing the motion of water particles for 45° inclination at 0.7 Hz.

At this point the vortex generated by the lip has drifted into the chamber and almost diminished. We can expect lower levels of circulating flow near the lip as the front wall becomes more parallel to the incoming wave direction i.e. when the inclination angle reduces. The water level has reached a maximum inside the chamber, as the free water surface velocity is almost zero; the particle will change their direction after this instant and the water level will drop in the chamber.

As the water level in the chamber falls, air is sucked into the OWC from the atmosphere as seen in Fig. 12. The purpose of the nozzle placed at the atmosphere was to create a pressure differential between the atmosphere and the turbine

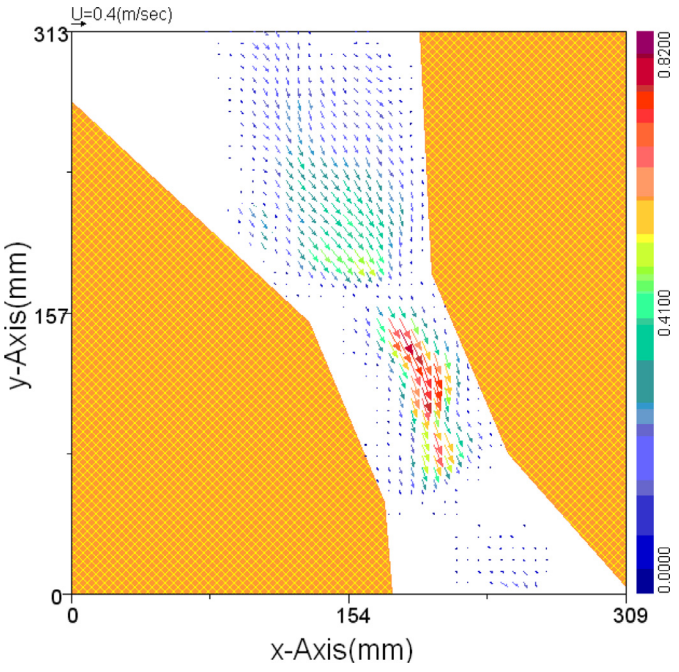

Fig. 12. Velocity vectors showing the motion of water particles for 75° inclination at 0.6 Hz during the inhalation stage.

section. The higher velocity vectors in the turbine section indicate this. Compared to a straight section this design will aid in reducing blade stall effects at low wave heights since the velocity is increased in the turbine section by the nozzles.

It should be noted that the velocity vectors are not visible in some areas in Figs. 10–12; this is because of the absence of the seed particles in those areas, as it proved a bit difficult to get the particles to all the regions of the flow especially the air flow due to its unique oscillating flow characteristics.

4. Conclusions

A new bend-free OWC was designed and its performance at different inclined positions and at the conventional vertical position is presented. The inclined OWC proved to be superior in performance with a marked increase in dynamic pressure at the turbine section. Water volume fluctuations in the chamber were also higher at lower inclination angles. An inclined OWC, typically angled between 45° and 55° will yield better output than a conventional vertical walled fixed OWC. This finding will help to design much more efficient OWC systems in future.

References

[1] W.N. Allsop, Wave Forces on inclined and Vertical Wall Structures, Task Committee of the Inclined and Vertical Wall Structures of the Committee on Waves and Wave Forces of the Waterway, Port Coastal and Ocean Division of the American Society of Civil Engineers, 1995, pp. 282–310.
[2] R. Bhattacharyya, M.E. McCormick, Elsevier Ocean Engineering Book Series, vol. 6, Elsevier, 2003, pp. 7–18.
[3] Y.M.C. Delaure, A. Lewis, Ocean Eng. 30 (2003) 309–330.

[4] D.G. Dorrell, W. Fillet, in: Proceedings of the International Conference on Energy and Environment (ICEE 2006), Selangor, Malaysia, 2006, pp. 23–32.
[5] A.F.D.O. Falcao, in: Proceedings of the Fourth European Wave Energy Conference, Aalborg, Denmark, 2000.
[6] A.F.D.O. Falcao, Renew. Sustain. Energy Rev. 14 (2010) 899–918.
[7] L.H. Holthuijsen, Waves in Oceanic and Coastal Waters, Cambridge University Press, United Kingdom, 2007, pp. 177–232.
[8] K. Horikawa, Coastal Engineering: An Introduction to Ocean Engineering, University of Tokyo Press, 1978, pp. 28–96.
[9] D.S. Jeng, Ocean Eng. 29 (2002) 1711–1724.
[10] W.M. Jentse, J.P.F.M. Janssen, Port Coastal and Ocean Division of the American Society of Civil Engineers, 1995, pp. 1–26.
[11] P.M. Koola, M. Ravindran, P.A.A. Narayana, ASCE J. Energy Eng. 121 (1995) 14–26.
[12] J. Kwon, W. Koo, in: Proceedings of the Twenty-third International Offshore and Polar Engineering Conference, Anchorage, Alaska, 30 June–5 July, 2013.
[13] M.A. Losada, F.L. Martin, R. Medina, Wave Kinematics and Dynamics in Front of Reflective Structures. Wave Forces on Inclined and Vertical Wall Structures, Task Committee of the Inclined and Vertical Wall Structures of The Committee on Waves and Wave Forces of the Waterway, Port Coastal and Ocean Division of the American Society of Civil Engineers, 1995, pp. 282–310.
[14] C.C. Lin, D.G. Dorrell, M.F. Hsieh, in: Proceedings of IEEE International Conference on Sustainable Energy Technologies, 2008.
[15] H. Maeda, T. Kinoshita, in: Proceedings of Hydrodynamics of Ocean wave Energy Utilization, IUTAM Symposium, Lisbon, Portugal, 1985.
[16] H. Maeda, S. Santhakumar, T. Setoguchi, M. Takao, Y. Kinoue, K. Kaneko, Renew. Energy 17 (1999) 533–547.
[17] Y. Masuda, M.E. McCormick, Wave to Energy Conversion, ASCE, 1978.
[18] M. Raffel, C. Willert, J. Kompenhans, Particle Image Velocimetry – A Practical Guide, first ed., Springer Verlag, Berlin, Heidelberg, 1998.
[19] K. Ram, M. Faizal, M.R. Ahmed, Y.H. Lee, J. Mech. Sci. Technol., 24, 2010, pp. 2043–2050.
[20] M. Rea, Wave Tank and Wavemaker Design: in *Ocean Wave Energy-Current Status and Future Perspectives*, Springer Verlag, Berlin, Heidelberg, 2008, pp. 147–159.
[21] A.J.N.A. Sarmento, Experiments in Fluids, Springer-Verlag, 1992.
[22] W.N. Seelig, in: Proceedings of Coastal Structure'83 Conference, Arlington, USA, American Society of Civil Engineers, New York, 1983, pp. 961–973.
[23] W.N. Seelig, J.P. Ahrens, Wave Reflection and Energy Dissipation by Coastal Structures. Wave Forces on Inclined and Vertical Wall Structures. Task committee of the Inclined and Vertical Wall Structures of the Committee on Waves and Wave Forces of the Waterway, Port Coastal and Ocean Division of the American Society of Civil Engineers, 1995, pp. 28–51.
[24] T. Setoguchi, S. Santhkumar, M. Takao, T.H. Tim, K. Kaneko, Renew. Energy 28 (2003) 79–91.
[25] W. Sheng, B. Flannery, A. Lewis, R. Alcorn, in: Proceedings of the ASME 2012 31st International Conference on Ocean, Offshore and Arctic Engineering, Rio de Janeiro, Brazil, July 1–6, 2012.
[26] K. Taira, Y. Nagata, J. Oceanogr. Soc. Jpn. 24 (1968) 242–252.
[27] [27]The Queens University of Belfast (2002), Islay Limpet Wave Power Plant, Publishable Report, 1st November 1998 to 30th April 2002, The Queens University of Belfast.
[28] M. Torresi, S.M. Camporeale, P.D. Stripoli, G. Pascazio, Renew. Energy 33 (2008) 735–747.
[29] V. Venugopal, G.H. Smith, Ocean Eng. 34 (2007) 1120–1137.
[30] World Energy Council, Survey of Energy Resources Executive Summary, World Energy Council, 2007, pp. 5–41.
[31] L. Zaoui, B. Bouali, S. Larbi, A. Benchatti, Energy Proc. 50 (2014) 246–254.